RNA (2000), *6*:668–679. Cambridge University Press. Printed in the USA.

Probing the structure of RNAIII, the *Staphylococcus aureus agr* regulatory RNA, and identification of the RNA domain involved in repression of protein A expression

YVONNE BENITO,[1] FABRICE A. KOLB,[2] PASCALE ROMBY,[2] GERARD LINA,[1] JEROME ETIENNE,[1] and FRANÇOIS VANDENESCH[1]

[1]EA1655, Faculté de Médecine Laennec, 69372 Lyon Cedex 08, France
[2]UPR 9002 du Centre National de la Recherche Scientifique, Institut de Biologie Moléculaire et Cellulaire, 67084 Strasbourg Cedex, France

ABSTRACT

RNAIII, a 514-nt RNA molecule, regulates the expression of many *Staphylococcus aureus* genes encoding exoproteins and cell-wall-associated proteins. We have studied the structure of RNAIII in solution, using a combination of chemical and enzymatic probes. A model of the secondary structure was derived from experimental data with the help of computer simulation of RNA folding. The model contains 14 hairpin structures connected by unpaired nucleotides. The data also point to three helices formed by distant nucleotides that close off structural domains. This model was generally compatible with the results of in vivo probing experiments with dimethylsulfate in late exponential-phase cultures. Toe-printing experiments revealed that the ribosome binding site of *hld*, which is encoded by RNAIII, was accessible to the *Escherichia coli* 30S ribosomal subunit, suggesting that the in vitro structure represented a translatable form of RNAIII. We also found that, within the 3′ end of RNAIII, the conserved hairpin 13 and the terminator form an intrinsic structural domain that exerts specific regulatory activity on protein A gene expression.

Keywords: *agr* locus; chemical and enzymatic probing; in vivo probing; regulation; RNAIII

INTRODUCTION

In *Staphylococcus aureus*, expression of several virulence factors is regulated by the global regulon *agr*. The *agr* system is composed of two divergent operons designated P2 and P3. The P2 operon combines a density-sensing cassette (*agrD* and *B*) and a two-component sensory transduction system (*agrA* and *C*), both of which are required for autocatalytic activation of the promoter P2 and for transcription from the divergent promoter P3 (Ji et al., 1995; Lina et al., 1998). The effector of the *S. aureus agr* system is a 514-nt transcript of the P3 operon, designated RNAIII, which contains the 26-amino-acid delta-hemolysin gene (*hld*). RNAIII stimulates the expression of postexponentially expressed extracellular toxins and enzymes such as alpha and beta-hemolysins, enzymes (lipases, proteases and nucleases) and toxins (toxic shock syndrome toxin and enterotoxins), and represses the expression of exponential-phase surface proteins such as protein A and coagulase. RNAIII appears to be the specific regulator, as cloned RNAIII, defective in delta-hemolysin production, and expressed in an RNAIII-deletion mutant, restored both the positive and negative effects on the expression of exoproteins and surface proteins (Janzon & Arvidson, 1990) and in an *agr*-null strain (Kornblum et al., 1990; Novick et al., 1993). RNAIII acts primarily on target gene transcription initiation and, in the case of alpha-hemolysin, independently stimulates translation by a mechanism that appears to involve direct interaction between the 5′ end of RNAIII and a stretch of approximately 80 bp within the ribosome binding site of the *hla* transcript (Morfeldt et al., 1995). The mechanism by which RNAIII controls the transcription of its target genes is unknown. One possibility is that RNAIII acts via *trans*-acting factors, as RNAIII is potentially capable of forming stable secondary structures that may create protein binding sites (Novick et al., 1993). The importance of the 5′ and 3′ regions of RNAIII for its regulatory function has been tested by deletion

Reprint requests to: Francois Vandenesch, EA1655, Faculté de Médecine Laennec, Rue Guillaume Paradin, 69372 Lyon Cedex 08, France; e-mail: denesch@univ-lyon1.fr.

analysis and by studying the ability of RNAIII homologs from non-*aureus* staphylococcal species to complement *agr*-deficient strains of *S. aureus* (Benito et al., 1998; Tegmark et al., 1998). The 3′ end of RNAIII may be important to repress protein A expression, and may therefore be an intrinsic domain (Novick et al., 1993; Benito et al., 1998). As mentioned above, besides its regulatory function, RNAIII is also an mRNA that encodes the delta-hemolysin gene. Translation of RNAIII into delta-hemolysin was delayed by 1 h following transcription and this delay was abolished by deletion of the 3′ half of RNAIII, suggesting that a conformational change of the RNA is required for translation (Balaban & Novick, 1995). Secondary structure predictions indicate that the 5′ and 3′ ends of RNAIII may pair, thereby sequestering the ribosomal binding site of *hld* (Novick et al., 1993). Taken together, these data indicate that the structure of RNAIII plays an essential role not only in *hld* translation but also in regulatory functions.

Here, we probed the secondary structure of *S. aureus* RNAIII in vitro, using chemical and enzymatic probes. The results were compared with those of in vivo probing of RNAIII produced during the late exponential phase. The proposed model of RNAIII secondary structure is characterized by 14 hairpin structures and three long-range interactions that bring the 3′ and 5′ ends of RNAIII into close proximity. A number of hairpin structures appear to be conserved within the *Staphylococcus* species. One, located in the 3′ end of *S. aureus* RNAIII, efficiently repressed protein A expression in vivo. The proposed model for the secondary structure of RNAIII is discussed in the light of its regulatory functions.

RESULTS

Structural probing of *Staphylococcus aureus* RNAIII

We investigated the conformation of RNAIII (nt 1–514) with various chemical and enzymatic probes (Ehresmann et al., 1987) (Fig. 1). We chose an identical pH, temperature, ionic strength, and divalent ion concentration for the different probes to minimize the effects of these parameters on conformational changes. The four bases were tested at one of their Watson–Crick pairing positions by using DMS (N1A > N3C) and CMCT (N3U > N1G). Single-stranded regions were probed with RNases T2 and T1, and helical regions were detected with the double-stranded specific RNase V1. Information on the 3′ and 5′ ends of RNAIII was obtained using enzymes, DMS (for N3C), and nickel complex (which modifies N7G). Nickel complex is sensitive to stacking of base rings; for example, the N7 position of a guanine within a helix is not reactive unless the deep groove is widened (Chen et al., 1993). The RNA molecules were renatured in the presence of magnesium ions prior to modification. We also verified that the RNAs folded into a homogenous population by using gel electrophoresis in nondenaturing conditions. A secondary structure model for RNAIII was derived from the experimental data with the help of a computer simulation of RNA folding (Gultyaev et al., 1995). This procedure folds the molecule by generating consecutive transitions between favorable intermediate structures, that is, by simulating folding pathways rather than by searching for the global minimum state (Gultyaev et al., 1995; Gerdes et al., 1997). The secondary structure model is characterized by 14 hairpin structures and three helices (A–C) which involve distant nucleotides (Fig. 2). The model can be divided into three mains domains: the 5′ end domain (nt 1–31), a central domain delimitated by helix B (nt 32–382) and the 3′ end domain (nt 383–514).

The 5′ end domain contains a well-characterized stem-loop motif. This hairpin structure 1 bears a GNRA loop that is known to adopt a particular structure closed by a sheared G-A base pair (Heus & Pardi, 1991; Pley et al., 1994). The poor accessibility of G9 and A12 towards chemicals and enzymes supports the existence of such a G-A base pair (Fig. 1A,E). Two long-range interactions involving residues A24-G30/U452-458 (helix C) and U32-A42/U371-G382 (helix B) can be proposed. Both helices are susceptible to RNase V1 hydrolysis and several nucleotides are weakly or not reactive at one of their Watson–Crick positions. However helix C presents a weak stability as evidenced by the concomitant presence of several single-strand-specific RNase cleavages (Fig. 2). Thus, helix C brings in close proximity the 3′ and 5′ domains whereas helix B delimitates the central domain.

In this large central domain, the reactivity patterns of nucleotides in hairpin 2–11 were characteristic of hairpin structures (Fig. 2), as most of the nucleotides located in the loops were reactive at their Watson–Crick positions. This was accompanied by single-strand-specific RNase cleavages (Figs. 1 and 2). Furthermore, the stems were all cleaved by RNase V1, and most of the nucleotides were weakly or not reactive towards chemicals. This is particularly well-illustrated for the stem-loop motifs 3, 4, 5, and 7–11 (Fig. 2). Helix 2, which is A-U rich, forms a metastable helical structure, which may account for the concomitant presence of RNase V1 and RNase T2 cleavages and for the reactivity of several nucleotides at Watson–Crick positions (Fig. 2). The long hairpin structure 6, characterized by a stem rich in A-U base pairs and interrupted by an internal loop, required magnesium for stabilization: most of the residues within the helix became strongly reactive in the absence of magnesium (Fig. 1B). The central domain also contained a branched structure constituted by hairpins 7–9 and closed by helix A (Fig. 2). This helix involving the two distant regions G207–U216 and A310–U319 is supported by the presence of sev-

eral RNase V1 cleavages in both strands, and by the nonreactivity of several residues towards chemicals (Figs. 1 and 2). The single-stranded conformation of the interhelical regions is supported mainly by the reactivity of nucleotides at their Watson–Crick position (Figs. 1 and 2). This was notably the case for nucleotides A42–U47, U65–A68, A105–A109, C138–C140, A157–U163, A218–A220, U258–A260, U321–U327, and U350–C353.

The 3′ end domain is constituted by three hairpins, 12–14, and by a long single-stranded region involving residues 459–483 (Fig. 2). The stem-loop structure 13 is clearly identified, but its folding required the presence of magnesium, because many nucleotides within the helix became reactive under semidenaturing conditions (Fig. 2D). The stem, rich in A-U base pairs, is interrupted by two bulged nucleotides and closed by a 13-nt long loop. Finally, hairpin 14, corresponding to the terminator, is rich in G-C base pairs and is one of the most stable stem-loops of RNAIII. Its existence is supported by the presence of RNAse V1 cuts on both sides of the helix, and by the fact that none of the cytosines at position N3 and the guanines at position N7 (located in the helix) were reactive towards chemicals (Fig. 1C). In addition, cytosines 495–496 and 498–500 at their N3 positions were highly reactive with DMS, and several RNase T2 cleavages occurred in the loop (Fig. 1C).

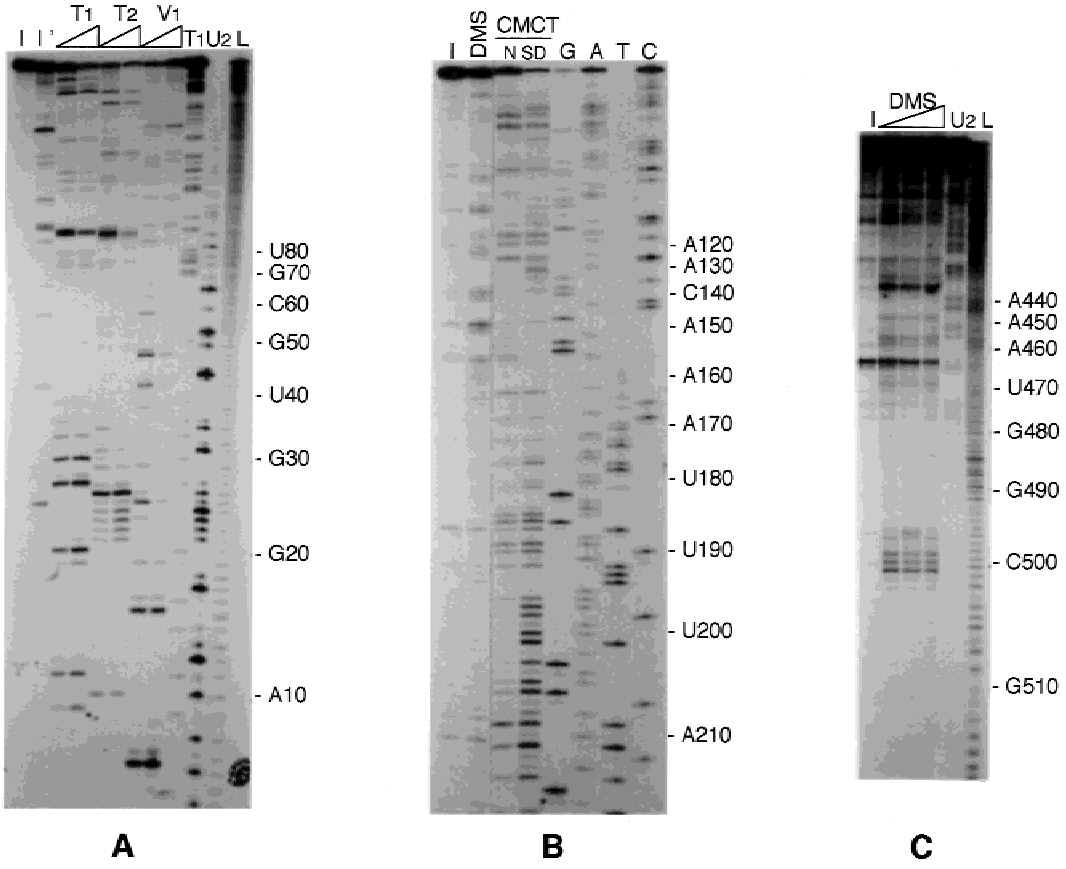

FIGURE 1. Probing the structure of RNAIII in vitro and in vivo. Selected autoradiograms showing enzymatic (**A**) and chemical (**B**,**C**) probing performed at 37 °C on in vitro transcribed RNAIII. **A**: RNase T1 (T1), RNase T2 (T2) and RNase V1 (V1) hydrolysis on 5′-labeled RNAIII, short migration. Lanes I, I′: incubation controls in buffer used for RNase T1, and RNase V1 hydrolysis, respectively; lanes T1: 0.05 and 0.15 U of RNase T1; lanes T2: 0.02 and 0.04 U of RNase T2; lanes V1: 0.1 and 0.2 U of RNase V1; lanes T1 and U2: RNases T1 and U2 in denaturing conditions, respectively; lane L: alkaline ladder. **B**: DMS and CMCT modifications, long migration. Lane I: incubation control in buffer used for DMS; lane DMS: native conditions, 1 μL of DMS diluted 1:16; lanes CMCT: native conditions (N) and semidenaturing conditions (SD), 2 μL of CMCT (100 mg/mL); lanes G, A, T, and C correspond to sequencing ladders. **C**: DMS modification of cytosines at N3 on 3′-end-labeled RNAIII, short migration. Lane I: incubation control; lanes DMS: native conditions, 1, 2, and 4 μL of DMS diluted 1:8; lanes U2 and L as in **A**. **D** and **E**: selected autoradiograms showing DMS and CMCT modifications on in vitro transcribed RNAIII (as in **B**) and a comparison with DMS modification on RNAIII in vivo, short migration. The differences in reactivities are denoted by arrows. Lanes I: incubation controls in buffer used for DMS; lanes DMS in vivo: 25 μL of DMS in 20 mL of staphylococcal culture at late exponential growth phase; lanes DMS in vitro: native conditions (N), semi-denaturing conditions (SD), 1 μL of DMS diluted 1:16; lanes CMCT: native conditions (N), semi-denaturing conditions (SD), 1 μL of CMCT (100 mg/mL); lanes G, A, T, and C correspond to sequencing ladders. (*Figure continues on facing page.*)

Probing the structure of the 3′ end of RNAIII

Because it had been suggested that the 5′ and 3′ ends of RNAIII would pair, and because specific regulatory activity was attributed to the 3′ end (Novick et al., 1993; Benito et al., 1998), the conformation of this region (nt 394–490) was probed separately with chemical and enzymatic probes (Fig. 3). Interestingly, the enzymatic cleavage and chemical reactivity patterns of nt 409–483 in the 3′ domain were identical to those in the entire RNAIII molecule and are thus consistent with the existence of stem-loop structure 13 (Figs. 2 and 3). Indeed, RNase V1 cuts occurred at positions 410–418, 421–422, 439, 443–444, and 447–450, whereas the main RNase T2 cleavage sites were located in the hairpin loop at positions 423–430 and 434–437 (Fig. 3). Furthermore, the nucleotides in the external loop were all highly reactive with chemical probes at their Watson–Crick position (Fig. 3). The presence of several RNase V1 cuts in the upper part of the stem (A419–U424/A438–U443) and the reactivity of several uridines pointed to the formation of a metastable helix.

The main reactivity changes observed between the entire RNAIII molecule and the 3′ end domain alone were located at nt U452–U466. Indeed, in the 3′ domain alone, all these nucleotides were reactive at one of their Watson–Crick positions and were cleaved by RNase T2 (Fig. 3A), indicating that this region is single stranded.

In vivo DMS probing of RNAIII

The structure of RNAIII was studied in vivo by using DMS, which alkylates cytosine at N3 and adenine at N1 (Mayford & Weisblum, 1989). In a typical experiment, *S. aureus* strain RN6390 was grown to the late exponential phase and treated with DMS. Sites of RNAIII modification were detected by the primer extension reaction on RNA extracts and were compared to modifications observed in vitro. As shown in Figure 1D,E, reactivity with RNAIII in vivo and in vitro was essentially identical, as only nucleotides in the hairpin loop and interhelical regions were highly sensitive to DMS. Differences between the in vitro and in vivo mapping data mainly concerned the reactivity of the adenine residues involved in the proposed long-range interactions, particularly helix B (U371–G382/U32–A42). These adenines were more sensitive to DMS alkylation at their N1 position in vivo than in vitro (Fig. 1D). Another sig-

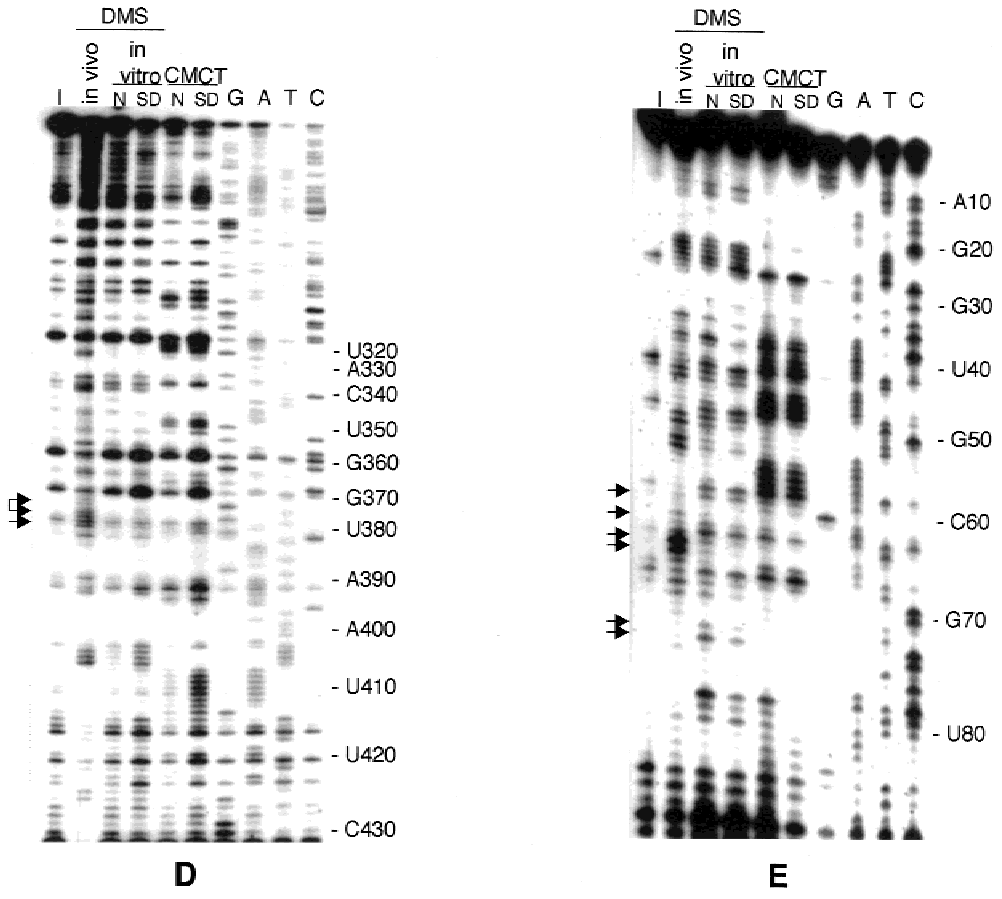

FIGURE 1. (*continued.*)

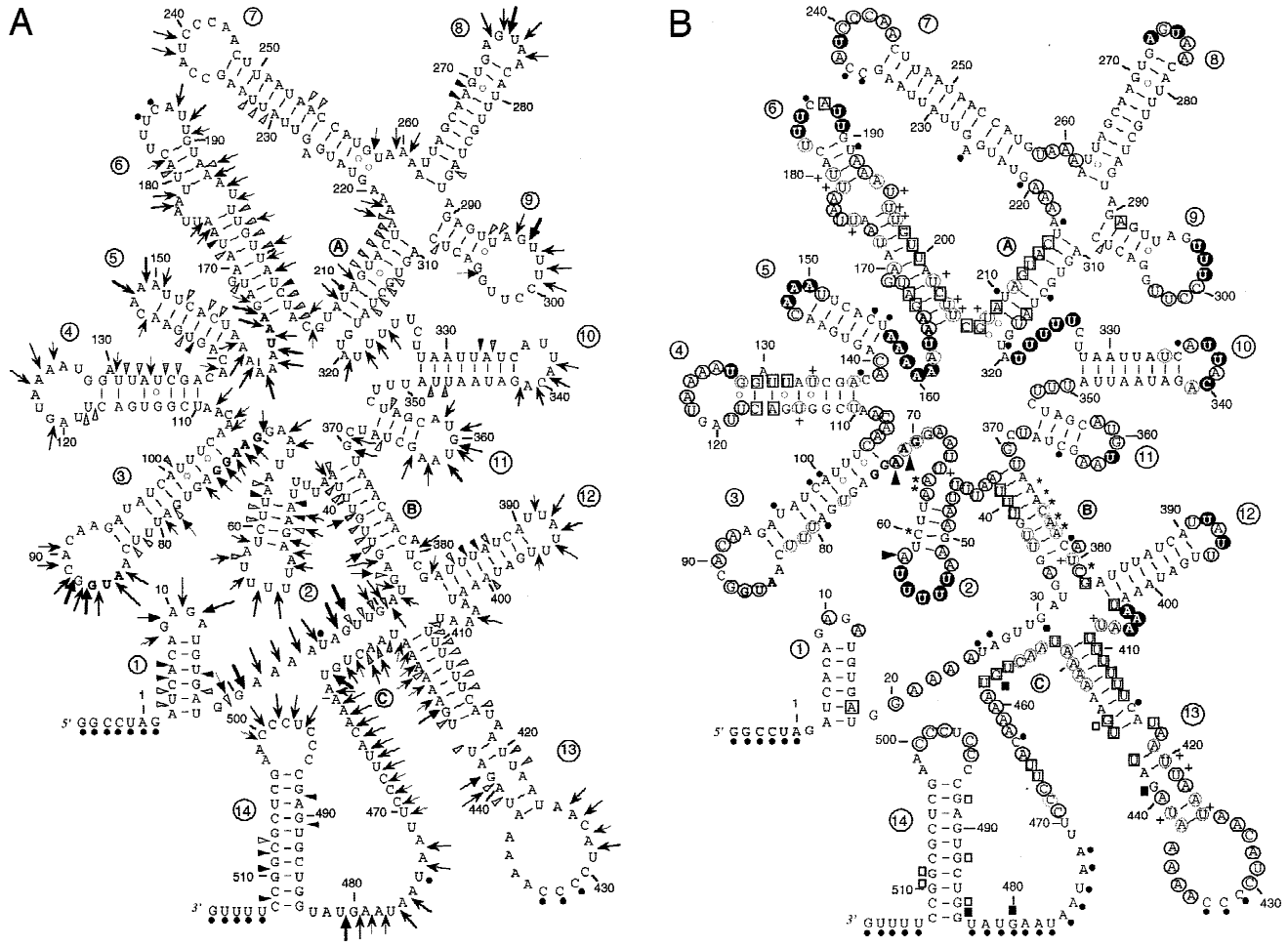

FIGURE 2. Secondary structure model of RNAIII showing the enzymatic cleavages (**A**) and reactivity of nucleotides to chemicals probes (**B**). The hairpin structures are numbered 1 to 14; long distance interactions are designated A, B and C; the Shine–Dalgarno sequence and the start and stop codons of *hld* are in bold face. **A**: RNase T1 cleavages are denoted by (→), RNase T2 by (→), thick, medium, or thin arrows for strong, moderate or low reactivity, respectively; RNase V1 cleavages are denoted by black, gray, or empty triangles for strong, moderate, or low reactivity, respectively. **B:** Reactivity of Watson–Crick positions to DMS (N1A, N3C) and CMCT (N3U, N1G) are represented as follows: reactive in native conditions (darkened black or grey circles for strong, moderate or low reactivity, respectively); reactive only in semidenaturing conditions (squares); more reactive in semidenaturing conditions (cross); nonreactive in both native and semidenaturing conditions (no symbol). Dots indicate not determined due to unspecific cleavages or pauses of RT in the incubation control. Guanines reactive at position N7 to NiCr are denoted by black squares, and empty squares denote unreactive guanines. Information about guanine accessibility at N7 position is only provided for region 410–512. The differences between the reactivity of adenine at N1 and cytosines at N3 to DMS in vitro and in vivo are indicated as follows: increased reactivity in vivo by an asterisk and protection in vivo by black triangles. These data were obtained from four independent experiments.

nificant difference between in vivo and in vitro mapping results concerned several adenine residues located at the ribosome initiation site. Indeed, adenines 58, 71, and 72 were clearly nonreactive in vivo, whereas adenines 58 and 57 became more reactive at their N1 positions in vivo (Figs. 1E, 2).

Ribosomes bind to *S. aureus* RNAIII

Although RNAIII is transcribed in the mid-exponential phase of growth, it is translated into delta-hemolysin only 1 h later (Balaban & Novick, 1995). This delay is not dependent on a specific timing signal during the growth cycle, and is abolished by deletion of the 3′ end of RNAIII (Balaban & Novick, 1995). We therefore probed the accessibility of the *hld* ribosome binding site in vitro by using a toe-printing assay (Hartz et al., 1988). In this primer extension inhibition assay, formation of the ternary complex composed of the 30S subunit, RNAIII, and the initiator $tRNA^{Met}$ blocks the elongation of a cDNA primer by reverse transcriptase (Hartz et al., 1988). Indeed, the 30S/$tRNA_f^{Met}$ complex incubated with the refolded RNAIII produced a strong

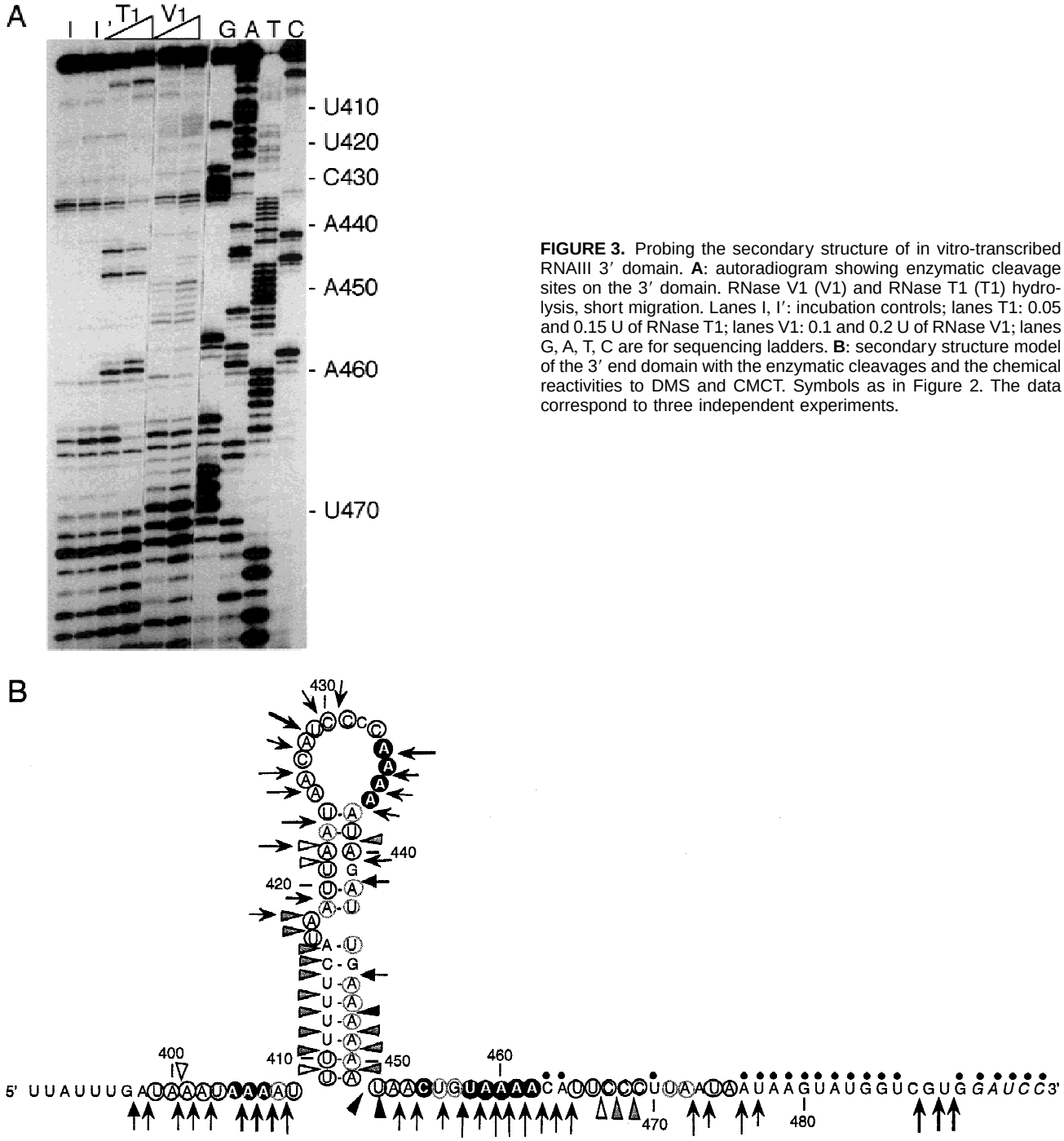

FIGURE 3. Probing the secondary structure of in vitro-transcribed RNAIII 3′ domain. **A**: autoradiogram showing enzymatic cleavage sites on the 3′ domain. RNase V1 (V1) and RNase T1 (T1) hydrolysis, short migration. Lanes I, I′: incubation controls; lanes T1: 0.05 and 0.15 U of RNase T1; lanes V1: 0.1 and 0.2 U of RNase V1; lanes G, A, T, C are for sequencing ladders. **B**: secondary structure model of the 3′ end domain with the enzymatic cleavages and the chemical reactivities to DMS and CMCT. Symbols as in Figure 2. The data correspond to three independent experiments.

toe-print at A100, 15 nt downstream of the initiation codon (Fig. 4), as previously shown (Hartz et al., 1988). The yield of the toe-print was identical when RNAIII was denatured prior to the experiment (Fig. 4). Given the possibility that the primer used for reverse transcription perturbed the structure of RNAIII, formation of the ternary 30S/RNAIII/tRNA^{Met} complex was also studied in filter binding assays (not shown). Again the data showed no major differences between native and denatured RNAIII. Altogether, these results indicate that ribosomes bind efficiently to *hld* RBS and that the in vitro structure represents a translatable form of RNAIII.

The 3′ domain of RNAIII represses protein A gene expression

We have shown here that the 3′ end of RNAIII is an independent structural domain. Furthermore, we and others have previously shown that the 3′ end of the

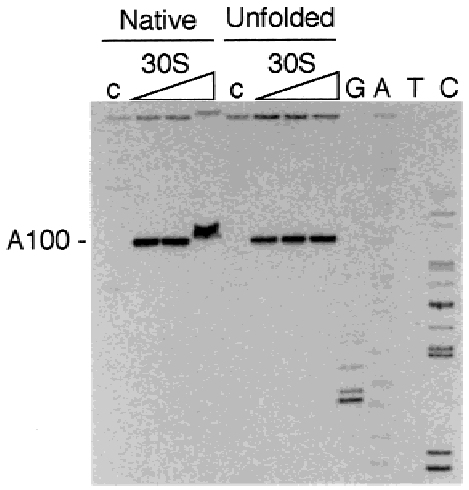

FIGURE 4. Accessibility of the ribosome binding site in RNAIII in vitro. The experiments were conducted in parallel on native and denatured (unfolded) RNAIII molecules. The position of the toeprint (A100) is indicated. Lane c: incubation control of free RNA in the presence of 30S subunit; lanes 30S: experiment in the presence of increasing concentrations of 30S subunits (125, 250 and 625 nM); lanes G, A, T and C are for sequencing ladders.

RNAIII is important for repressing protein A gene (*spa*) expression, and may thus be a functional domain (Novick et al., 1993; Benito et al., 1998). To further investigate this question, we subcloned selected fragments of RNAIII under the control of the RNAIII promoter on the staphylococcal plasmid pE194 and introduced the resulting constructs in *S. aureus* strain WA400 (*agr*$^-$, lacking RNAIII). Down regulation of *spa* expression was achieved normally in WA400/pE194 expressing either the RNAIII fragment comprising residues 391–514 (Fig. 5, lane 4) or residues 403–455 and 484–514 (both RNA fragments contain hairpin 13 and the terminator) (Fig. 5, lane 5). Interestingly, WA400/pE194 expressing a fragment of RNAIII that contains only the transcription terminator (nt 484–514) was still able to repress *spa* expression, albeit to a lesser extent (Fig. 5, lane 3).

DISCUSSION

The secondary structure model of *S. aureus* RNAIII

S. aureus RNAIII regulates the expression of several genes encoding exoproteins and cell-wall-associated proteins (Novick et al., 1993). RNAIII also encodes delta-hemolysin, but inactivation of the open reading frame does not affect the regulatory function of RNAIII (Janzon & Arvidson, 1990; Novick et al., 1993). There is also evidence that RNAIII may undergo conformational changes that activate either its translation or its regulatory functions (Novick et al., 1993; Balaban & Novick, 1995). A computer-simulated model of the secondary structure of RNAIII has been proposed (Novick et al., 1993). This model was based on minimum energy solutions and was characterized by extensive long-range interactions between the 5′ and 3′ domains (Novick et al., 1993). This prompted us to analyze the conformation of RNAIII in vitro by using several chemical and enzymatic probes, and in vivo by using DMS. These experimental data formed the basis for a secondary structure model derived with the help of computer simulation of RNAIII folding (Gultyaev et al., 1995). The present secondary structure of RNAIII is characterized by a number of hairpin structures (Fig. 2), most of which had been predicted (Novick et al., 1993; Tegmark et al., 1998). We also bring evidence that most of these stem-loop structures occurred in vivo. The alignment of RNAIII from *S. aureus* with that of non-*aureus* staphylococcal species (*S. epidermidis*, *S. warneri*, *S. simulans*, and *S. lugdunensis*) reveals that the stem-loop motifs 1, 7, 13, and 14 are predicted to be highly conserved by computer folding, and the hairpins 6, 8, 9, 11, and 12 must be present in all RNAIII but their sequences diverged (Vandenesch et al., 1993; Tegmark et al., 1998). Interestingly, several base pair compensatory changes are found in helices 1, 7, 13, and 14 among *Staphylococcus* species (Fig. 6). Thus the high conservation of hairpins 1, 7, 13, and 14 suggests a common function. For instance, with the exception of *S. epidermidis* RNAIII, which carries a 5-nt-long loop (Fig. 6), hairpin 1 contains a conserved GAGA loop motif. It is well known that stable stem-loop structures located at the 5′ end of mRNA may increase its stability (for a review, see Bechhofer, 1993). It is therefore tempting to propose a 5′ stabilizer function for this conserved hairpin motif in

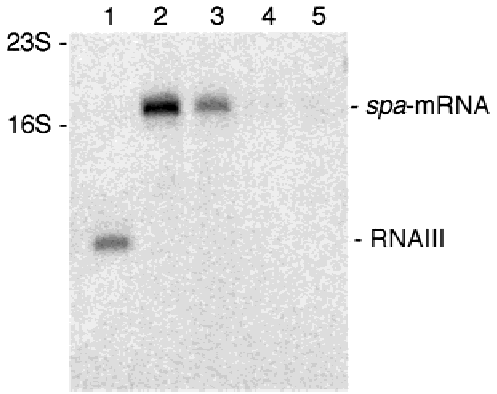

FIGURE 5. Effect of truncated RNAIII on protein A gene transcription. Northern blot analysis of RNAIII and protein A mRNA expression. RNAs from postexponential phase cultures were hybridized with probes corresponding to RNAIII and protein A gene (*spa*). Lane 1: RN6390 (*agr*$^+$); lane 2: WA400 (*agr* mutant); lane 3: WA400/pLUG310 (terminator transcription alone, nt 484–514); lane 4: WA400/pLUG300 (3′ end RNAIII, nt 391–514); lane 5: WA400/pLUG315 (hairpin structure 13 transcription terminator, nt 403–455::484–514). RNAIII transcripts are not seen in lanes 4 and 5 because of their very small sizes. Positions of migration of 16S rRNA (1541 nt) and 23S rRNA (2904 nt) indicated.

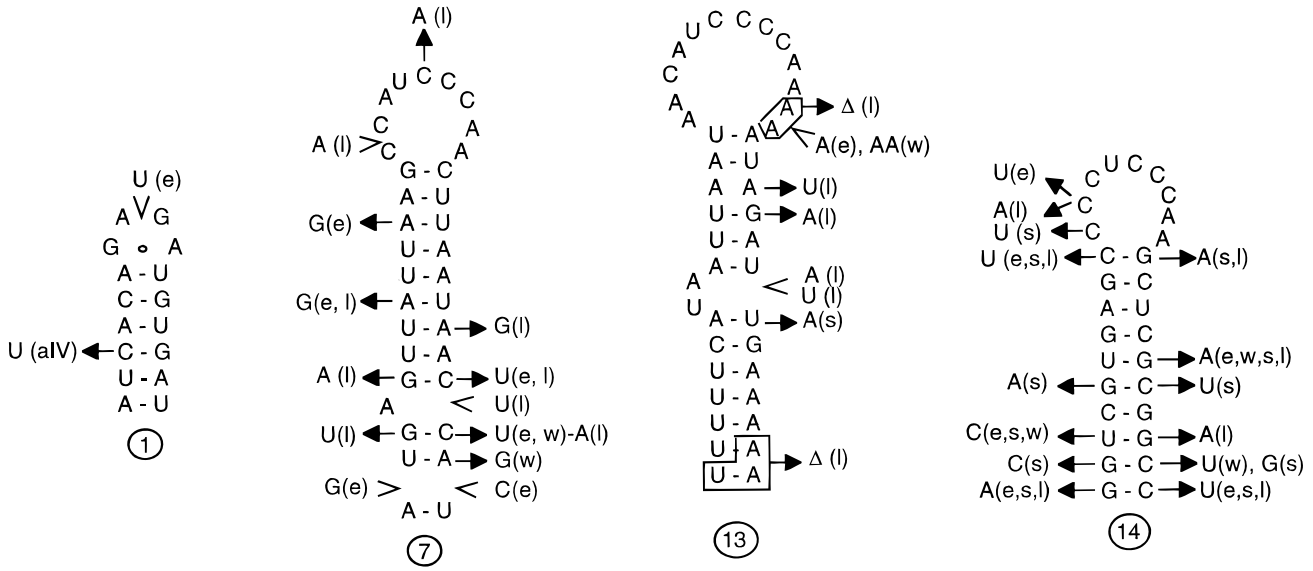

FIGURE 6. Sequence of several conserved hairpin structures of RNAIII from *S. aureus* (types I–IV), and comparison with four different species, *S. epidermidis* (e), *S. warneri* (w), *S. simulans* (s), and *S. lugdunensis* (l). Nucleotide insertion is shown by an open arrow, and Δ is for deletion. The hairpin structures have been assigned according to the secondary structure model presented in Figure 2.

RNAIII. The central domain (nt 32–382) is closed by helix B (Fig. 2). Analogous long-range interaction may also arise in *S. epidermidis*, *S. simulans*, and *S. warneri* as suggested by computer folding, despite the fact that the sequence is not conserved (data not shown). The central domain encloses the open reading frame encoding for delta-hemolysin that is present in all RNAIII, except *S. lugdunensis*, with a high degree of sequence identity (Vandenesch et al., 1993; Tegmark et al., 1998). The central domain also contains a branched structure constituted by three hairpins, 7–9, closed by a long-range interaction (helix A). The existence of helix A, which was clearly demonstrated in vitro, was also supported by the in vivo probing. In this branched structure, hairpin 7 is of particular interest. Several base pair compensatory changes are found among *Staphylococcus* species, and the loop contains a conserved sequence (UCCCAA) that resembles that of the loops of hairpin 13 and the terminator (Fig. 6). This high conservation indicates that hairpin 7 is a potential recognition site for *trans*-acting factor(s).

The central domain may undergo specific conformational changes

The 5′ side of the central domain of RNAIII contains the regulatory region (nt 19–87) involved in the activation of alpha-toxin translation (Novick et al., 1993; Morfeldt et al., 1995). Binding of RNAIII to the leader region of alpha-toxin mRNA induced a conformational change of the *hla* mRNA, rendering the ribosomal initiation site available for translation (Morfeldt et al., 1995). In the proposed model of RNAIII, the two long-range interactions B and C hide part of the *hla*-mRNA binding sequence, indicating that conformational changes of RNAIII are required for efficient binding. Interestingly, the greater accessibility of adenines 372–378 in vivo suggests that helix B is destabilized, likely as the result of *hla* mRNA binding to the 5′ region of RNAIII, explaining the apparent discrepancy with the in vitro data. Different pairing pathways that result in the formation of stable antisense RNA and mRNA complexes have been described (for a review, see Zeiler & Simons, 1998). In most cases, binding initiates between two loops, or between a loop and a single-stranded RNA segment involving a restricted number of nucleotides, and more stable complexes are subsequently formed by pairing of distal RNA segments. In region 42–72 of RNAIII, several nucleotides show high accessibility to single-strand-specific probes, indicating that they are potential sites for initial pairings. A fragment of RNAIII containing nt 1–380, which potentially forms helix B, is indeed competent for binding to *hla* mRNA in vitro (Morfeldt et al., 1995).

The central domain also contains the ribosomal initiation site required for the translation of delta-hemolysin, which is the only known translation product of RNAIII. Thus, the two functions of RNAIII (translation of *hld* and translational regulation of *hla*) are mutually exclusive. Structural probing of RNAIII in vitro revealed that the RBS sequence and the AUG initiation codon of *hld* are both accessible to single-strand-specific probes. The toe-printing and filter binding assays showed that the ribosome efficiently binds both to native RNAIII and to the denatured molecule at the *hld* initiation site (Fig. 4).

Footprinting experiments indicated that the initiating ribosome protects ~40–50 nt (Murakawa & Nierlich, 1989; Huttenhofer & Noller, 1994). As the 3′ side occurred at position +15 from the adenine of the initiation codon (as determined by the toe-printing approach), we assume that the ribosome may cover part of stem-loop structure 2 from the 5′ side. Many groups have investigated the effects of RNA structure on translation initiation (e.g., for a review, see de Smit & van Duin, 1994). However, chemical probing indicated that stem-loop structure 2 is metastable, and the ribosome is thus able to bind to the unfolded form. It was also shown that a 5-bp hairpin located 3 nt upstream of the SD sequence of the T4 *rIIB* gene can be increased to 9 bp without having an inhibitory effect (Shinedling et al., 1987). Therefore, our data indicate that the in vitro structure of RNAIII corresponds to its translatable form. One intriguing finding is that translation of *hld* in vivo is delayed by 1 h following transcription (Balaban & Novick, 1995). It was postulated that a conformational change of RNAIII to a translatable form preceded its regulation of target genes (Balaban & Novick, 1995). This apparently conflicts with the fact that the in vitro structure is efficiently recognized by the ribosome. It is possible that, owing to transcription–translation coupling, some transient inhibitory structures occurring in vivo sequester the ribosome binding site or influence the kinetic folding pathway of RNAIII in vivo. Interestingly, the overall pattern of nucleotide reactivity to chemical probes was very similar in vivo and in vitro. One major difference was located within the RBS: in particular, the two adenines (71 and 72) of the Shine–Dalgarno sequence became protected in vivo (Fig. 2), a phenomenon which may correlate with occupancy by the ribosome of its initiation *hld* binding site. Indeed, in the initiation complex, base-specific protection mainly occurs in the RBS and at the initiation codon, reflecting the formation of stable base pairings with the 3′ end of 16S rRNA and the anticodon sequence of the $tRNA_f^{Met}$, respectively (Huttenhofer & Noller, 1994). However, in vivo probing of RNAIII took place in the late exponential phase of growth when RNAIII is also involved in transcriptional regulation of target genes. It is likely that RNAIII undergoes specific conformational changes that are necessary for defined functions. Thus, several populations of RNAIII may coexist in vivo but are difficult to distinguish by chemical mapping.

The 3′ end domain is sufficient for the control of protein A expression

We also identified an intrinsic structural domain in the 3′ end of RNAIII, with hairpin 13 at its center. Stem-loop 13 has been predicted to be partially base paired with the region encompassing nt 130–98 (Novick et al., 1993). However, structural mapping of the full-length RNAIII and of the RNAIII domain from nt 391–490 showed an almost identical nucleotide reactivity pattern, a finding consistent with the existence of a stem-loop motif, as further supported by the in vivo probing (Fig. 3). The stem of hairpin 13 is interrupted by two bulged residues (U417 and A418). Despite the apparently lower stability of the upper stem, the probing data point to the existence of a 13-nt-long loop (Fig. 2). Moreover, this 3′ domain exerted specific regulatory activity, as the last 124 nt cloned downstream of the P3 promoter in an RNAIII-deficient strain were sufficient to repress *spa* expression (Fig. 6). It is remarkable that only hairpin 13 (nt 403–455) and the terminator hairpin (nt 484–514) were required for efficient *spa* transcription control, as deletion of the conserved residues U456 to U489 did not affect regulation (Fig. 2). It has previously been shown that RNAIII from *S. lugdunensis* does not repress *spa* transcription, while a chimeric construct consisting of the 5′ end of *S. lugdunensis* RNAIII and the 3′ end of *S. aureus* RNAIII repressed *spa* expression more efficiently in a *S. aureus* background (Benito et al., 1998). Several sequence differences were observed between *S. lugdunensis* and *S. aureus* RNAIII in the hairpin loop of the terminator and stem-loop 13 (Fig. 6). Conversely, other coagulase-negative staphylococci in which the last 150 nt of RNAIII (including stem-loop 13, Fig. 6) are more strongly conserved were able to repress *spa* expression (Tegmark et al., 1998). These data point to a shared function of the 3′ end domain of several RNAIII species in *spa* regulation. We also found that the last 31 nt of RNAIII (containing the transcription terminator) partially repressed *spa* expression, suggesting that the terminator also participates in the regulatory mechanism. Whether the 3′ domain regulates transcription directly or indirectly is unknown. One plausible explanation is that hairpin 13 and the terminator of RNAIII act via a ribonucleoprotein complex. A possible role of RNA in modulating the activity of DNA binding proteins has been reported (Retallack & Friedman, 1995; Sledjeski & Gottesman, 1995). It is also noteworthy that both hairpin loops contain a conserved CCCAA sequence that may provide a bipartite protein binding site (Fig. 6).

In summary, RNAIII has the unique property of acting as a messenger RNA and having pleiotropic regulatory functions. The secondary structure model of RNAIII proposed here should help to clarify functional domains. We demonstrated here that the 3′ domain of RNAIII contains an independent structure and has a regulatory function in protein A synthesis.

MATERIALS AND METHODS

Bacterial strains and growth conditions

Escherichia coli TG1 and *S. aureus* RN4220, a nitrosoguanidine-induced mutant capable of accepting *E. coli* DNA (Kreiswirth et al., 1983), were used for plasmid amplification

and genetic manipulations. *S. aureus* RN6390 derives from 8325-4 and is our standard *agr*$^+$ strain. *S. aureus* WA400 is a derivative of 8325-4 in which the P2 operon is functional but the P3 operon is deleted and replaced by the chloramphenicol transacetylase gene (*cat86*) (Janzon & Arvidson, 1990) (see Table 1). Staphylococci were grown either on BM agar plates (1% peptone, 0.5% yeast extract, 0.1% glucose, 0.5% NaCl, 0.1% K_2HPO_4), or in brain-heart infusion (BHI), with erythromycin (5 μg mL^{-1}) when appropriate.

Molecular cloning and plasmid construction

Total DNA and plasmid DNA were prepared with standard methods (Sambrook et al., 1989). Transformation of *E. coli* TG1 was performed with cells rendered competent by treatment with $CaCl_2$, and *S. aureus* RN4220 and WA400 were transformed by electroporation (Bio-Rad gene pulser).

RNAIII was expressed in *Staphylococcus* by using plasmid pE194 (Horinouchi & Weisblum, 1982), which had been modified by adding an *Eco*RV restriction site next to the *Xba*I site forming pLUG274. PCR was performed from the RN6390 *agr* sequence (GenBank accession number X52543). To clone the 3′ domain of RNAIII under control of the P3 promoter, the promoter sequence was amplified using primers agr-sa1819/Stu1569 (Table 2), and the 3′ end of RNAIII was amplified using primers agr-sa757/Stu1180. The PCR products were digested by *Stu*I and ligated together before being reamplified with the external primers agr-sa1819 and agr-sa757. The resulting PCR product was digested with *Hin*dII and *Xba*I (site present on each primer) and ligated to the modified pE194 vector digested by *Eco*RV and *Xba*I. The ligation product was electroporated to RN4220 and the resulting plasmid (pLUG300) was introduced into strain WA400. To express intramolecular sequences of RNAIII under the control of the P3 promoter, we constructed, using a similar method, plasmid pLUG310 that contained the P3 promoter region linked to the transcriptional terminator (amplified using primers Bam1081 and agr-sa757); these two regions were separated by a short cloning sequence that contained the restriction sites *Stu*I and *BamH*I. To express hairpin structure 13 under the control of the P3 promoter, the corresponding sequence (nt 1168–1116) was amplified using primers Stu1168 and Bam1116, digested by *Stu*I and *BamH*I, and ligated to pLUG310 digested by the same enzymes.

For in vitro transcription, the RNAIII coding sequence (corresponding to nt 1–514 of RNAIII) was amplified using primers Stu1572 and Bam1055. The PCR product was digested by *Stu*I and *Bam*HI and ligated to the pUT7 vector (Serganov et al., 1997) cleaved with the same restriction enzymes. The resulting plasmid was introduced by transformation in *E. coli* TG1. Similarly, the 3′ end of RNAIII (nt 391–490) lacking the transcription terminator was amplified by using primers Stu1180 and Bam1079 and was then cloned onto pUT7 vector in *E. coli* TG1.

Northern blots

Electrophoresis of total RNA through 1% agarose gel containing 2.2 M formaldehyde, vacuum transfer to nylon membrane, hybridizations with specific digoxigenin-labeled RNA probes and luminescent detection were carried out as described (Benito et al., 1998). PCR primers for the production of *agr* RNAIII and protein A-specific gene probes were selected from GenBank accession number X52543 and A04518 respectively.

Preparation of RNA

RNAIII and the 3′ domain of RNAIII were transcribed in vitro with T7 RNA polymerase from *Bam*HI linearized pLUG322 and pLUG281, respectively. Transcription of RNAIII yielded a run-off product of 522 nt including five additional nucleotides at the 5′ end and three at the 3′ end, which all came from the vector. The 3′ domain corresponded to nt 391–490 of RNAIII.

TABLE 1. Main characteristics of strains and plasmids.

Strains or plasmids	Relevant characteristics	Reference or source
S. aureus strains		
8325-4	NCTC8325 cured of three prophages	Novick, 1963
RN4220	restriction-mutant of 8325-4	Kreiswirth et al., 1983
RN6390	derivative of 8325-4, *agr* positive	Peng et al., 1988
WA400	8325-4 Δ RNAIII region::*cat*86	Janzon & Arvidson, 1990
LUG450	WA400/pLUG300	this work
LUG460	WA400/pLUG310	this work
LUG467	WA400/pLUG315	this work
E. coli plasmids		
pUT7	pUC119::T7 promoter	Serganov et al., 1997
PLUG322	pUT7::RNAIII nt 1–514	this work
pLUG281	pUT7::RNAIII nt 391–490	this work
Staphylococcal plasmids		
pE194	3.728 kb *S. aureus* plasmid, inducible MLS resistance (*erm*)	Horinouchi & Weisblum, 1982
pLUG300	pE194::P3 promoter link to 3′-end RNAIII (nt 391–514)	this work
PLUG310	pE194::P3 promoter-TT (nt 484–514)	this work
pLUG315	pLUG310::hairpin 13 (nt 403–455)	this work

TABLE 2. Oligonucleotides.

Primer sense (+/−)	Position on *agr* sequence[a]	Position on RNAIII sequence[b]	5′-to-3′ sequence[c,d]	Restriction site
agr-sa757 (+)	757–771	—	AAC**GTT**AACGCGAAAATATAC	*Hin*dII
agr-sa1819 (−)	1819–1805	—	TTT**CT**AGATACGTGGCAAAC	*Xba*I
Stu 1569	1569–1588	—	CTG**AGGC**CTAGTTATATTAAAACATGC	*Stu*I
Bam1081 (−)	1087–1068	484–503	**ATA**GGA**TCC**GAGCCCCTCCCAAG	*Bam*HI
Stu1168 (−)	1168–1144	403–427	TGA**GGCC**TAAAATTTTTTTCATAATTAATAAC	*Stu*I
Bam1116 (+)	1116–1133	455–438	GT**GGAT**CC**C**GTTATTTTTTCAATCTAT	*Bam*HI
Stu1572 (−)	1572–1560	1–11	TA**GGC**CTAGATCACAGAG	*Stu*I
Stu1180 (−)	1180–1161	391–410	T**AGG**CC**T**TATTTGATAAATAAAATTT	*Stu*I
Bam1079 (+)	1081–1094	490–477	AGGG**ATC**CACGACCATACTTA	*Bam*HI
Bam1055 (+)	1055–1065	505–516	TCA**GG**A**TCC**AAAAGGCCGCG	*Bam*HI
agr-sa1329 (+)	1329–1350	242–221	GGGATGGCTTAATAACTCATAC	—
agr-sa1101 (+)	1101–1120	470–451	AGGGAATGTTTTACAGTTAT	—

[a] According to GenBank sequence X52543.
[b] According to the direction of transcription (nt 1 of RNAIII (A) corresponds to nt 1570 (T) of the *agr* sequence).
[c] Restriction sites underlined.
[d] Additional nucleotides in bold.

In vitro transcribed RNAs were purified by 8% polyacrylamide-8 M urea gel electrophoresis. After elution in 0.5 M ammonium acetate/1 mM EDTA buffer, the RNAs were precipitated twice with ethanol.

To prepare RNAs with free 5′-OH groups, the in vitro transcription step using T7 RNA polymerase was performed in the presence of 4 mM ApG, and 1 mM NTPs according to Pitulle et al. (1992). 5′-end labeling of RNA or DNA oligonucleotides was performed with T4 polynucleotide kinase and [γ-^{32}P]ATP (Sambrook et al., 1989). 3′-end labeling of RNA was performed with T4 RNA ligase and [^{32}P]-pCp (England & Uhlenbeck, 1978). Labeled RNAs or DNA were purified by 8% polyacrylamide/8 M urea gel electrophoresis, eluted and precipitated twice with ethanol. Before use, the different RNAs were renatured by incubation at 90 °C for 2 min in RNase-free water, followed by slow cooling at 20 °C in the buffer used for enzymatic hydrolysis or chemical modifications (see below).

Enzymatic probing

Enzymatic hydrolysis was performed on either 50,000 cpm of end-labeled RNAIII or 2 pmol of cold RNA in 10 μL of TMN buffer (20 mM Tris-acetate, pH 7.5, 10 mM Mg-acetate, 100 mM sodium-acetate), in the presence of 1 μg of carrier tRNA at 20 °C for 5 min with one of the following enzymes: RNase T1 (0.005 and 0.01 U), RNase V1 (0.1 and 0.05 U) or RNase T2 (0.05 U).

Chemical probing

Chemical modifications were performed on 2 pmol of RNAIII or of the 3′ domain at 20 °C in 20 μL of reaction buffer containing 2 μg of carrier tRNA. Alkylation of the C(N3) and A(N1) positions was done with 1 μL DMS (diluted 1/8 and 1/16 in ethanol) for 2 min in TMN buffer. Modification of U(N3) and G(N1) were done with 5 μL of CMCT (100 mg/mL) for 15 min in a buffer containing 50 mM Na-borate, pH 8, 5 mM MgAc, 150 mM KOAc. DMS and CMCT reactions were also carried out in semi-denaturing conditions in the same buffers containing 1 mM EDTA instead of magnesium and KOAc.

When using end-labeled RNA, cleavage at modified C residues was induced by hydrazine subsequently followed by aniline treatment (Peattie & Gilbert, 1980). Modification of G(N7) by NiCR was performed at 20 °C for 30 min according to Chen et al. (1993) in a volume of 20 μL containing 25 mM phosphate-KOH pH 7.0, 10 mM $MgCl_2$, 100 mM NaCl, 2 μg carrier tRNA, in the presence of 3 μM NiCr and 200 μM $KHSO_5$. Cleavage at modified G residues was induced by aniline treatment (Peattie & Gilbert, 1980).

Identification of cleavage and modification sites

End-labeled RNA fragments were sized on 12% polyacrylamide/8 M slab gels. Cleavage positions were identified by running RNase T1, RNase U2 and alkaline ladders of the RNA in parallel (Donis-Keller et al., 1977). The cleavage or modification sites of unlabeled RNAs were detected by primer extension. The modified RNAs were hybridized with 4 pmol of 5′-end-labeled DNA primers agr-sa1101 (complementary to nt 470–451) or agr-sa1329 (complementary to nt 242–221). Details for hybridization conditions, primer extension and analysis of the data have been described previously (Brunel et al., 1991).

In vivo DMS modification of RNA

Late log-phase cultures of RN6390 (OD_{540} = 1.5) were treated with 25 and 50 μL of DMS for 5 min at 37 °C according to Mayford and Weisblum (1989). Reactions were stopped by adding 10 mL of cold 10 mM Tris-HCl, pH 8.0, 5 mM EDTA buffer. The cells were then pelleted, treated with lysostaphine (50 μg/mL) and 1% SDS. Total RNA was extracted with an equal volume (500 μL) of phenol/chloroform saturated in 0.1 M Na-acetate pH 4, precipitated with ethanol and resuspended in RNase-free water to a final concentration of 2 mg/mL. Primer extension was carried out with 5 μg of RNA as described above.

Toe-printing experiments

The formation of a simplified translational initiation complex and the extension inhibition conditions were strictly identical to those described by Moine et al. (1990). 30S subunits were prepared from tight couples according to a procedure adapted from Makhno et al. (1988). Relative toe-printing (toe-print band over 5′ ends + toe-print) was calculated by scanning the gel with a Bio-imager Analyzer BAS 2000 (Fuji).

ACKNOWLEDGMENTS

We thank G. Wagner, S. Arvidson, R.P. Novick, H. Moine, C. Ehresmann, and B. Ehresmann for stimulating discussions. This work was supported in part by grants from Centre National de la Recherche Scientifique (CNRS).

Received December 10, 1999; returned for revision February 3, 2000; revised manuscript received February 28, 2000

REFERENCES

Balaban N, Novick RP. 1995. Translation of RNAIII, the *Staphylococcus aureus agr* regulatory RNA molecule, can be activated by a 3′-end deletion. *FEMS Microbiol Lett 133*:155–161.

Bechhofer D. 1993. 5′ mRNA stabilizers. In: Belasco JG, Brawerman G, eds. *Control of messenger RNA stability*. London: Academic Press. pp 31–52.

Benito Y, Lina G, Greenland T, Etienne J, Vandenesch F. 1998. *Trans*-complementation of a *Staphylococcus aureus agr* mutant by *Staphylococcus lugdunensis agr* RNAIII. *J Bacteriol 180*:5780–5783.

Brunel C, Romby P, Westhof E, Ehresmann C, Ehresmann B. 1991. Three-dimensional model of *Escherichia coli* ribosomal 5 S RNA as deduced from structure probing in solution and computer modeling. *J Mol Biol 221*:293–308.

Chen X, Woodson SA, Burrows CJ, Rokita SE. 1993. A highly sensitive probe for guanine N7 in folded structures of RNA: Application to tRNA(Phe) and Tetrahymena group I intron. *Biochemistry 32*:7610–7616.

de Smit MH, van Duin J. 1994. Control of translation by mRNA secondary structure in *Escherichia coli*. A quantitative analysis of literature data. *J Mol Biol 244*:144–150.

Donis-Keller H, Maxam AM, Gilbert W. 1977. Mapping adenines, guanines, and pyrimidines in RNA. *Nucleic Acids Res 4*:2527–2538.

Ehresmann C, Baudin F, Mougel M, Romby P, Ebel JP, Ehresmann B. 1987. Probing the structure of RNAs in solution. *Nucleic Acids Res 15*:53–71.

England TE, Uhlenbeck OC. 1978. 3′-terminal labelling of RNA with T4 RNA ligase. *Nature 275*:560–561.

Gerdes K, Gultyaev AP, Franch T, Pedersen K, Mikkelsen ND. 1997. Antisense RNA-regulated programmed cell death. *Annu Rev Genet 31*:1–31.

Gultyaev AP, van Batenburg FH, Pleij CW. 1995. The computer simulation of RNA folding pathways using a genetic algorithm. *J Mol Biol 250*:37–51.

Hartz D, McPheeters DS, Traut R, Gold L. 1988. Extension inhibition analysis of translation initiation complexes. *Methods Enzymol 164*:419–425.

Heus HA, Pardi A. 1991. Structural features that give rise to the unusual stability of RNA hairpins containing GNRA loops. *Science 253*:191–194.

Horinouchi S, Weisblum B. 1982. Nucleotide sequence and functional map of pE194, a plasmid that specifies inducible resistance to macrolide, lincosamine, and streptogramin type B antibiotics. *J Bacteriol 150*:804–814.

Huttenhofer A, Noller HF. 1994. Footprinting mRNA-ribosome complexes with chemical probes. *EMBO J 13*:3892–3901.

Janzon L, Arvidson S. 1990. The role of the delta lysin gene in the regulation of virulence genes by the accessory gene regulator (*agr*) in *Staphylococcus aureus*. *EMBO J 9*:1391–1399.

Ji G, Beavis RC, Novick RP. 1995. Cell density control of staphylococcal virulence mediated by an octapeptide pheromone. *Proc Natl Acad Sci USA 92*:12055–12059.

Kornblum J, Kreiswirth B, Projan SJ, Ross H, Novick R. 1990. *Agr*: a polycistronic locus regulating exoprotein synthesis in *Staphylococcus aureus*. In: Novick RP, ed. *Molecular biology of the staphylococci*. New York: VCH Publishers. pp 373–401.

Kreiswirth B, Lofdahl S, Betley M, O'Reilly M, Schlievert P, Bergdoll M, Novick RP. 1983. The toxic shock syndrome exotoxin structural gene is not detectably transmitted by a prophage. *Nature 305*:709–712.

Lina G, Jarraud S, Ji G, Greenland T, Pedraza A, Etienne J, Novick RP, Vandenesch F. 1998. Transmembrane topology and histidine protein kinase activity of AgrC, the *agr* signal receptor in *Staphylococcus aureus*. *Mol Microbiol 28*:655–662.

Makhno VI, Peshin NN, Semenkov Iu P, Kirillov SV. 1988. A modified method of isolation of "tight" 70S ribosomes from *Escherichia coli* highly active at different stages of the elongation cycle. *Mol Biol* (Mosk) *22*:670–679.

Mayford M, Weisblum B. 1989. Conformational alterations in the *ermC* transcript in vivo during induction. *EMBO J 8*:4307–4314.

Moine H, Ehresmann B, Romby P, Ebel JP, Grunberg-Manago M, Springer M, Ehresmann C. 1990. The translational regulation of threonyl-tRNA synthetase. Functional relationship between the enzyme, the cognate tRNA and the ribosome. *Biochim Biophys Acta 1050*:343–350.

Morfeldt E, Taylor D, von Gabain A, Arvidson S. 1995. Activation of alpha-toxin translation in *Staphylococcus aureus* by the *trans*-encoded antisense RNA, RNAIII. *EMBO J 14*:4569–4577.

Murakawa GJ, Nierlich DP. 1989. Mapping the *lacZ* ribosome binding site by RNA footprinting. *Biochemistry 28*:8067–8072.

Novick RP. 1963. Analysis by transduction of mutations affecting penicillinase formation in *Staphylococcus aureus*. *J Gen Microbiol 33*:121–136.

Novick RP, Ross HF, Projan SJ, Kornblum J, Kreiswirth B, Moghazeh S. 1993. Synthesis of staphylococcal virulence factors is controlled by a regulatory RNA molecule. *EMBO J 12*:3967–3975.

Peattie DA, Gilbert W. 1980. Chemical probes for higher-order structure in RNA. *Proc Natl Acad Sci USA 77*:4679–4682.

Peng HC, Novick RP, Kreiswirth B, Kornblum J, Schlievert PM. 1988. Cloning, characterization, and sequencing of an accessory gene regulator *agr* in *Staphylococcus aureus*. *J Bacteriol 170*:4365–4372.

Pitulle C, Kleineidam RG, Sproat B, Krupp G. 1992. Initiator oligonucleotides for the combination of chemical and enzymatic RNA synthesis. *Gene 112*:101–105.

Pley HW, Flaherty KM, McKay DB. 1994. Model for an RNA tertiary interaction from the structure of an intermolecular complex between a GAAA tetraloop and an RNA helix. *Nature 372*:111–113.

Retallack DM, Friedman DI. 1995. A role for a small stable RNA in modulating the activity of DNA-binding proteins. *Cell 83*:227–235.

Sambrook J, Fritsch E, Maniatis T. 1989. *Molecular cloning: A laboratory manual*. Cold Spring Harbor, New York: Cold Spring Harbor Laboratory Press.

Serganov A, Rak A, Garber M, Reinbolt J, Ehresmann B, Ehresmann C, Grunberg-Manago M, Portier C. 1997. Ribosomal protein S15 from *Thermus thermophilus*: Cloning, sequencing, overexpression of the gene and RNA-binding properties of the protein. *Eur J Biochem 246*:291–300.

Shinedling S, Gayle M, Pribnow D, Gold L. 1987. Mutations affecting translation of the bacteriophage T4 rIIB gene cloned in *Escherichia coli*. *Mol Gen Genet 207*:224–232.

Sledjeski D, Gottesman S. 1995. A small RNA acts as an antisilencer of the H-NS-silenced *rcsA* gene of *Escherichia coli*. *Proc Natl Acad Sci USA 92*:2003–2007.

Tegmark K, Morfeldt E, Arvidson S. 1998. Regulation of *agr*-dependent virulence genes in *Staphylococcus aureus* by RNAIII from coagulase-negative staphylococci. *J Bacteriol 180*:3181–3186.

Vandenesch F, Projan S, Kreiswirth B, Etienne J, Novick R. 1993. *Agr*-related sequences in *Staphylococcus lugdunensis*. *FEMS Microbiol Lett 111*:115–122.

Zeiler BN, Simons RW. 1998. Antisense RNA structure and function. In: Simons RW, Grunberg-Manago M, eds. *RNA structure and function*. Cold Spring Harbor, New York: Cold Spring Harbor Laboratory Press. pp 437–464.